3
B meson anomalies

3.1 Introduction

It is well known that the standard model of electroweak-interactions cannot be considered as the ultimate theory of fundamental interactions of nature. The theory can be extended in two ways (i) direct search and (ii) indirect search. In direct search, collider experiments search for new particles. But, till date there is no such direct evidence of beyond SM particles from the currently running experiments. On the other hand, the indirect search enables us to probe new physics through the observed phenomena which have deviations from the SM predictions. In particular, the rare decay modes of mesons can play a very crucial role. In fact, we already have signatures of new physics in measurements related to decays of B mesons. Interestingly most of these measurements are in semi-leptonic decays of B mesons:

- Flavour changing neutral current (FCNC) transition $b \to s\, l^+\, l^-$ ($l = e,\ \mu$): Lepton-flavor universality (LFU) is a symmetry deeply embedded in the SM and hence its violation will lead to the discovery of new physics. The LFU observables can be constructed by comparing the same observable for processes differing only in the lepton flavor involved. For example, in the context of $b \to s\, l^+\, l^-$, one can consider the ratio of the branching ratios of decays induced by $b \to s\, \mu^+\, \mu^-$ *vs.* $b \to s\, e^+\, e^-$. The Large Hadron Collider Beauty (LHCb) collaboration reported deviations from LFU in $b \to s\, l^+\, l^-$ sector [42, 47, 49]. These measurements are indication of new physics in $b \to s\, e^+\, e^-$ and/or $b \to s\, \mu^+\, \mu^-$. Further, there are anomalies independent of LFU violation. These are in decays $B^0 \to K^{0*}\, \mu^+\, \mu^-$ and $B_s \to \phi\, \mu^+\, \mu^-$ [40, 41, 43–46, 48] which is related to possible new physics in $b \to s\, \mu^+\, \mu^-$ transition.

- Charged current transition $b \to c\, l\, \bar{\nu}$ ($l = e,\ \mu,\ \tau$): The observed anomalies in this sector are related to LFU violation [51–59]. These are indications of possible new physics in $b \to c\, \tau\, \bar{\nu}$.

In this chapter, we discuss anomalous measurements in these sectors.

3.2 Experiments at the B-factories and at the LHC

In this section, we briefly discuss some of the current and future experimental facilities related to the measurements of observables in the B meson sector. The B meson observables are measured in two extremely different experimental environments:

- e^+e^- colliders: The two different e^+e^- accelerators, BaBar at SLAC, US [38] and Belle at KEKB, Japan [39] were approved in 1993 and 1994, respectively. These accelerators are basically e^+e^- circular colliders chosen to operate at the center-of-mass energy of 10.58 GeV corresponding to the invariant mass of the $\Upsilon(4S)$ resonance. This resonance particle decays either into a B^+B^- or a $B^0\bar{B}^0$ pair, and hence serves as a copious source of B mesons. Due to this reason, these accelerator facilities are popularly known as B factories. Another e^+e^- facility, the Belle II experiment [140] is upgraded from the Belle detector and is designed to take data with a 40 times higher event rates. Thus the B factories collect a large data sample of B decays in a very clean environment.

- pp collider: The Large Hadron Collider (LHC) at the European Organisation for Nuclear Research (CERN) is a pp collider housed in the 27 km toric tunnel at a depth of about 100 m underground which was bored in 1984-1989 for the LEP collider. It is designed to accelerate beams of protons in ultra-high vacuum up to an energy of 7 TeV travelling in opposite directions. The two beams are crossed at four specific interactions points around the ring resulting in a centre of mass energy of 14 TeV. These points are home to the four major experiments ALICE [175], ATLAS [17], CMS [18] and LHCb [37]. The final beam energy of 7 TeV is achieved though two of the LHC's pre-accelerators, the Proton Synchrotron (PS) [176] and Super Proton Synchrotron (SPS) [177, 178]. A schematic view of the LHC along with the four experiments are shown in Fig. 3.1. The CMS and ATLAS are general purpose experiments with primary focus on studying high transverse momentum particles and look for new physics signals through their 4π solid angle coverage. However, they also have a wide ranging bottom and top quark physics program. On the other hand, the LHCb experiment primarily focuses on studies related to bottom quark physics.

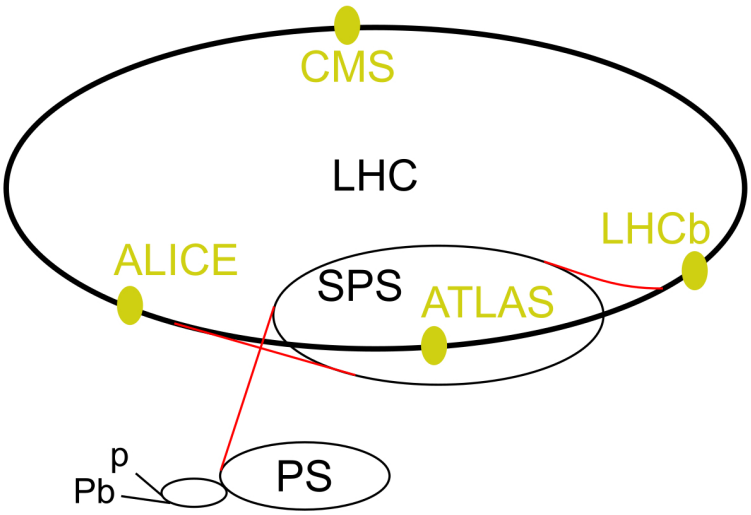

Figure 3.1: The LHC experiments and the pre-accelerators. Source:Wikipedia

In the following, we discuss some of the experiments relevant for B meson studies.

3.2.1 The BaBar experiment

The BaBar detector [38] operated at the PEP-II asymmetric e^+e^- collider at the SLAC National Accelerator Laboratory from 22 October 1999 to 7 April 2008. It was designed to operate at a center of mass energy of 10.58 GeV, the invariant mass of the $\Upsilon(4S)$ resonance which decays exclusively to B^+B^- and $B^0\bar{B}^0$ pairs and hence provided an ideal laboratory for the study of B meson physics. The primary physics goal of the BABAR experiment was detailed studies of CP-violating asymmetries in the decays of B mesons. However, it also focused on the precision measurements of decays of bottom and charm mesons along with τ leptons.

In PEP-II, the electron beam of 9 GeV and positron beam of 3.1 GeV collide head-on. This results in a Lorentz boost to the $\Upsilon(4S)$ resonance of $\beta\gamma$ = 0.56 which allows to reconstruct the decay vertices of the two B mesons. The interaction region is surrounded by the BaBar detector which is cylindrical with the interaction region at the center. The longitudinal section of the BaBar detector is shown in Fig. 3.2. In order to detect the particles, a series of sub detectors are arranged cylindrically around the interaction region. The inner detector consists of a silicon vertex tracker, a drift chamber, a ring-imaging Cherenkov detector, and a CsI electromagnetic calorimeter. These subdetectors are surrounded by a superconducting solenoid that produces a 1.5 T field inside the detector. This bends the tracks of charged particles allowing determination

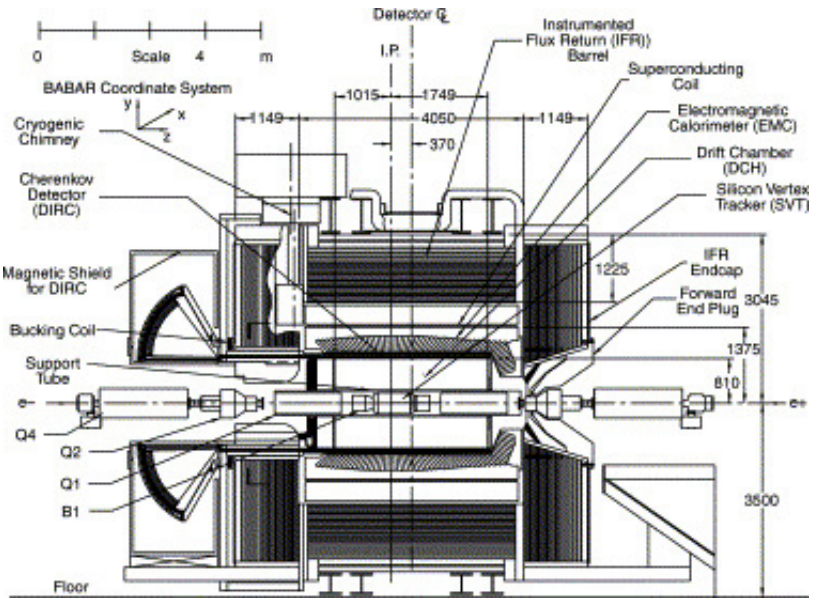

Figure 3.2: The longitudinal section of the BaBar detector [38].

of their momentum. Instrumented flux return is designed to detect muons and neutral hadrons. The BaBar experiment recorded a total integrated luminosity of 513 fb^{-1} during its entire run between 22 October 1999 to 7 April 2008.

3.2.2 The Belle experiment

The Belle experiment consists of the KEKB accelerator and the Belle detector which are located at the High Energy Accelerator Research Organization (KEK) in Tsukuba, Japan. The KEKB accelerator comprises of a linear accelerator and a main ring of 3 km circumference. The electrons produced by a thermal electron gun are accelerated to 8 GeV in the linear accelerator and then injected to the main ring. In order to produce positrons, a part of the electrons are collided with the tungsten target in the middle of the Linac. These positrons are collected and accelerated to 3.5 GeV and then injected to the main ring. These e^+ and e^- beams are collided at the interaction point in the TSUKUBA experimental hall where the Belle detector is located.

Belle detector surrounds the interaction point of the KEKB accelerator. Longitudinal cross-section of the Belle detector is shown in Fig. 3.3. It consists of several sub detectors. The silicon vertex detector (SVD) and the central drift chamber (CDC) are used to reconstruct trajectories of charged particles whereas the neutral particles can be detected in the electromagnetic calorimeter (ECL). The time-of-flight (TOF) counter and the aerogel Cherenkov counter (ACC) provide particle identification information of charged hadrons and electrons. A good distinction between pions and kaons momenta in the range of 100 MeV/c to a few GeV/c can be achieved. The extreme forward calorimeter (EFC), made up of CsI(Tl) scintillating crystals, is used as the instantaneous luminosity monitor. A superconducting solenoid magnet, providing a magnetic field of 1.5 T surrounds all inner sub-detectors. After the magnet and hence at the outermost part of the Belle detector, the KLM system is located which identifies the neutral K_L mesons and muons.

The data is collected at $\sqrt{s}$ = 10.58 GeV which is the invariant mass of the $\Upsilon(4S)$ resonance which decays into a pair of B mesons. The particles produced due to decays of B mesons are detected by the Belle detector. The KEKB accelerator was operative from 1999 to 2010. During this runtime several improvements such as crab cavities [180] were installed. These modifications led to a new world record instantaneous luminosity of $\mathcal{L} = 2.11 \times 10^{34}\,\mathrm{cm}^{-2}\mathrm{s}^{-1}$ and the total integrated luminosity of 1041 fb^{-1}. The data set contains 7.71×10^8 $B\bar{B}$ pairs. The KEKB was shut down in 2010 and since then, the KEKB has been upgraded

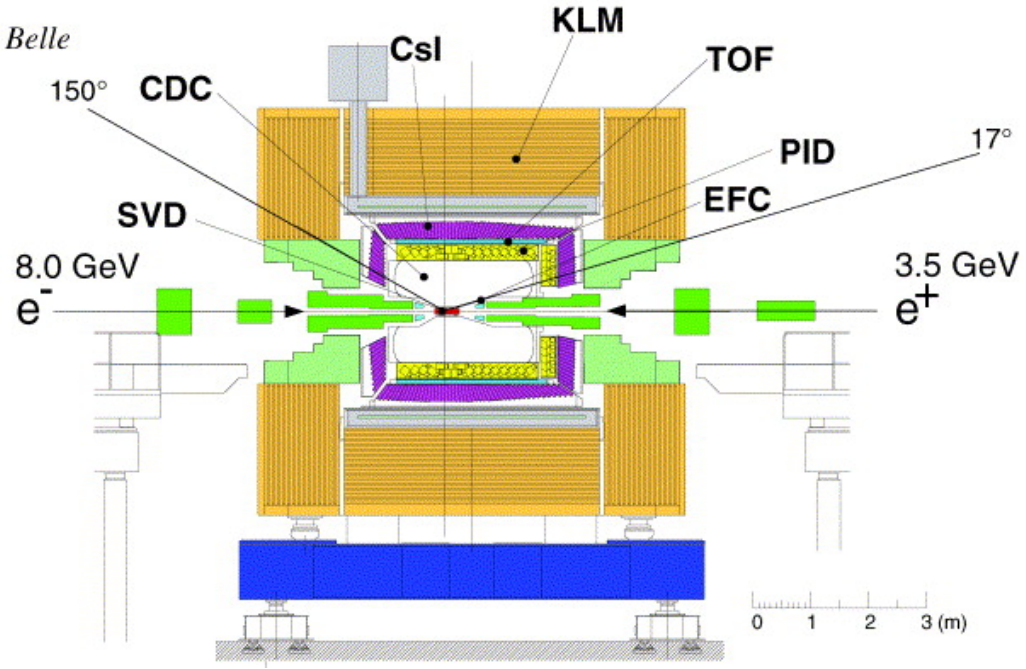

Figure 3.3: Longitudinal cross-section of the Belle detector [179].

to the SuperKEKB with up to 40 times increased luminosity for the Belle-II experiment.

3.2.3 The Belle-II experiment

The Belle-II experiment at the SuperKEKB accelerator at KEK, Tsukuba Japan is a two-ring energy-asymmetric electron-positron collider which is designed to collect data at the center of mass energy corresponding to the invariant mass of the Υ resonances. It an upgrade from its predecessor, the Belle experiment. e^- and e^+ are accelerated by a Linac up to 7.007 GeV and 4.000 GeV, respectively. The electrons storage link is called the high energy ring (HER) whereas the positrons storage range is called the low energy ring (LER). These rings are crossed at the interaction point at which the Belle-II detector is placed. The design luminosity of the SuperKEKB is $8 \times 10^{35}\,\mathrm{cm}^{-2}\mathrm{s}^{-1}$ which is about 40 times more than KEKB. It is expected to collect data corresponding to an integrated luminosity of 50 ab^{-1} which is approximately 50 times larger than the Belle experiment.

3.2.4 The LHCb experiment

The LHCb experiment primarily focuses on the study decays of B mesons. However, its physics programme also covers the charm, strange and top quark physics. The LHCb is a a forward detector as the $b\bar{b}$ pairs produced in the pp collision are heavily boosted either in the forward direction of the beam axis. Owing to the fact that LHCb is a forward arm spectrometer, the pseudorapidity η, defined as $\eta = -\ln(\tan(\theta/2))$, is limited in the range [2, 5]. Here θ is the angle between the beam axis and the particle momentum. However, this boost of the $b\bar{b}$ pairs allows to correctly identify the decay particles from each B meson and hence helps in reducing the background. Moreover, it also facilitates the commissioning and maintenance of the detector [181, 182].

A side view of the LHCb detector along with subdetectors are shown in Fig. 3.4. Various subdetectors of the LHCb detector propagate transversely along and radially out from the intersection point. The Vertex Locator (VELO) which is located closest to the interaction point, at a minimum distance of 8 mm, is a silicon micro-strip detector which measures the trajectories of particles that originate at the primary vertex. Apart from reconstructing the primary vertex, it also reconstructs the secondary vertices where heavy

hadrons such as B mesons decay. The next is the first of two Ring IMage CHerenkov (RICH) detectors which are designed to distinguish proton, charged pions and charged kaons through the Cherenkov effect whereby a radiation is emitted when a charged particle passes through a dielectric medium with a speed which is greater than the speed of light in that medium. RICH1 uses aerogel and fluorobutane. After this the particle passes through a strong magnetic field which bends the trajectories of the charged particles which can be seen in the tracking stations: Silicon Tracker (ST) and the Tracking Turnices (TT). Located after the tracking stations is the second RICH detector, RICH2 which uses CH_4 to cover a different momentum range in comparison to RICH1. The electromagnetic calorimeter (ECAL) and the hadronic calorimeter (HCAL) provide information about the energy of the particles. The ECAL is used for the charged particles and photons whereas HCAL is suitable for hadrons. These are located between the first and remaining muon stations. Finally there are five muon stations. The first one, M1, is between the RICH2 and the calorimeters.

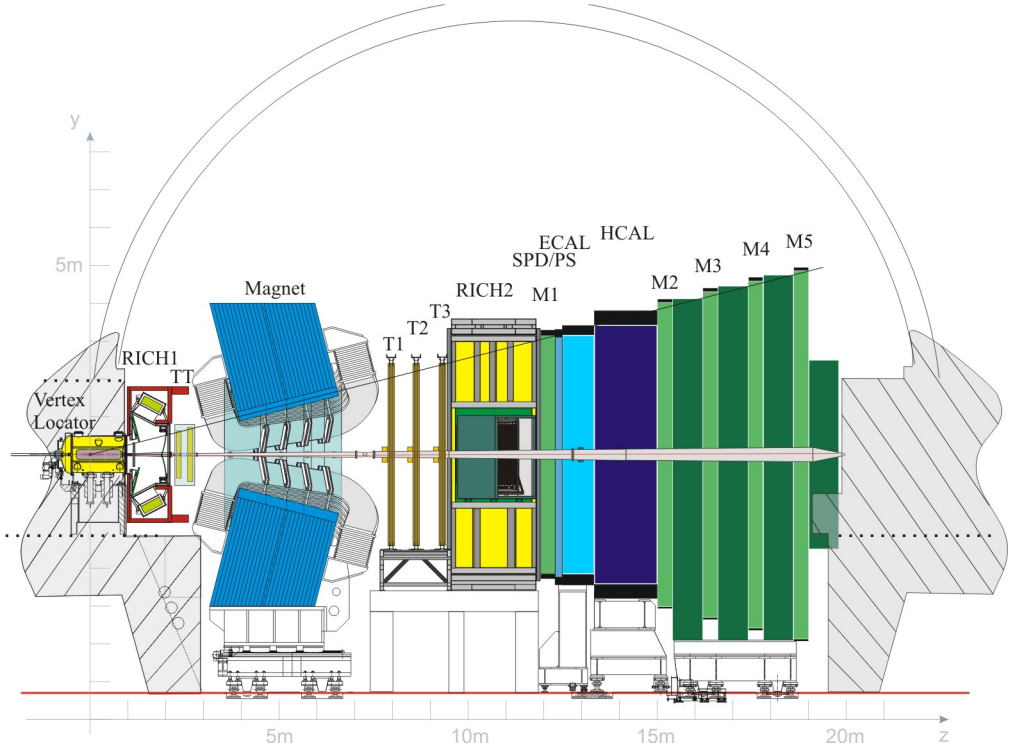

Figure 3.4: A schematic side view of the LHCb detector. Source: Wikipedia

In comparison to the electron-positron collider experiments such as Belle, the luminosity at the LHCb experiment is lower. However, the $b\bar{b}$ cross section is significantly higher at the LHCb resulting in larger total datasets of $b\bar{b}$ candidates. Moreover due to the environment created due to the pp collision, the background at LHCb is more polluted in comparison to that of the B-factories.

3.3 Anomalies in $b \to s\, l^+\, l^-$ sector

The $b \to s\, l^+\, l^-$ ($l = e$ or μ) decays occur only at loop level in the SM and hence are highly suppressed. There are several anomalous measurements, reported by LHCb experiment, related to the FCNC transitions $b \to s\, l^+\, l^-$. In this sector, the LFU violating ratios are defined as

$$R_K = \frac{\Gamma(B \to K^+\, \mu^+\, \mu^-)}{\Gamma(B \to K^+\, e^+\, e^-)}, \quad R_{K^*} = \frac{\Gamma(B \to K^*\, \mu^+\, \mu^-)}{\Gamma(B \to K^*\, e^+\, e^-)}\,. \tag{3.1}$$

In 2014, the LHCb collaboration reported the first measurement of the ratio R_K. The LHCb collaboration [42], from Run I analysis, reported the measurement of R_K to be $0.745^{+0.090}_{-0.074}\,(\text{stat.}) \pm 0.036\,(\text{syst.})$

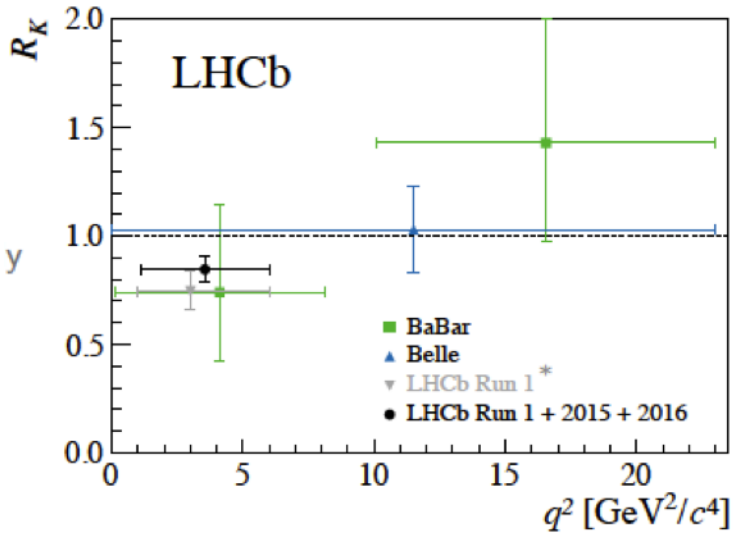

Figure 3.5: The R_K anomaly [183].

in the q^2 range $1.0 \leq q^2 \leq 6.0$ GeV^2, where q^2 is the invariant mass squared of the dilepton. Very recently, they have updated it including their Run II data [49]. The current combined measurement from both the runs is $R_K = 0.846^{+0.060}_{-0.054}\,(\text{stat.})^{+0.016}_{-0.014}\,(\text{syst.})$ which deviates from the SM prediction, $R_K\,(\text{SM}) \simeq 1$ [184, 185], by 2.5σ. The measurements of R_K from various experiments are depicted in Fig. 3.5 [183].

In 2017, the LHCb collaboration observed LFU violation in the ratio R_{K^*}. R_{K^*} was measured in two different q^2 bin which are [47]

$$\begin{aligned} R_{K^*} &= 0.660^{+0.110}_{-0.070}\,(\text{stat.}) \pm 0.024\,(\text{syst.}), \quad 0.045 \leq \text{q}^2 \leq 1.1\,\text{GeV}^2 \\ &= 0.685^{+0.113}_{-0.069}\,(\text{stat.}) \pm 0.047\,(\text{syst.}), \quad 1.1 \leq \text{q}^2 \leq 6.0\,\text{GeV}^2. \end{aligned} \tag{3.2}$$

The SM predicts $R_{K^*}\,(\text{SM}) \simeq 0.93$ at low q^2, but $R_{K^*}\,(\text{SM}) \simeq 1$ [184, 185] elsewhere. The measure-

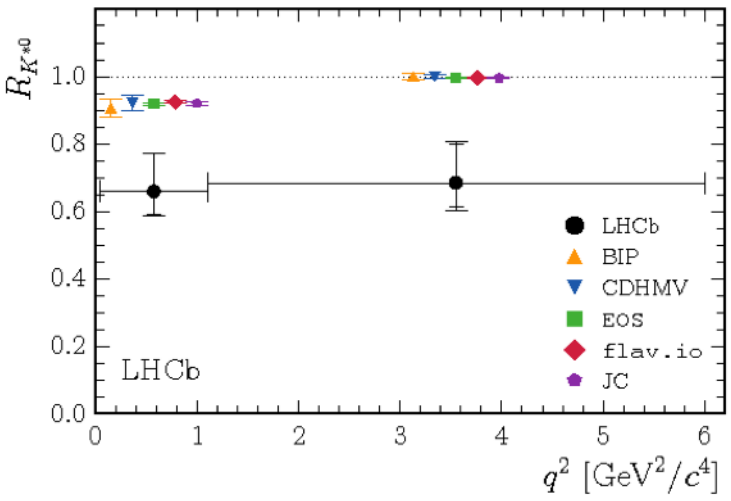

Figure 3.6: The R_{K^*} anomaly [186].

ments differ from the SM predictions by $2.2 - 2.4\sigma$ for low q^2 and $2.4 - 2.5\sigma$ for central q^2. Very recently Belle collaboration has reported their first measurements of R_{K^*} for both B^0 and B^+ modes in multiple q^2

bins [50]. These measurements are listed Table 3.1. It is obvious that Belle measurements have comparatively large uncertainties. Hence the anomaly in R_{K^*} still stands at the level of $\approx 2.5\sigma$. Measurements of R_{K^*}, superimposed to SM predictions are shown in Fig. 3.6 [186].

q^2 in GeV^2	B^0 modes	B^+ modes
[0.045, 1.1]	$0.46^{+0.55}_{-0.27} \pm 0.07$	$0.62^{+0.60}_{-0.36} \pm 0.10$
[1.1, 6.0]	$1.06^{+0.63}_{-0.38} \pm 0.13$	$0.72^{+0.99}_{-0.44} \pm 0.18$
[0.1, 8]	$0.86^{+0.33}_{-0.24} \pm 0.08$	$0.96^{+0.56}_{-0.35} \pm 0.14$
[15, 19]	$1.12^{+0.61}_{-0.36} \pm 0.10$	$1.40^{+1.99}_{-0.68} \pm 0.11$
[0.045, $q^2_{\rm max}$]	$1.12^{+0.27}_{-0.21} \pm 0.09$	$0.70^{+0.24}_{-0.19} \pm 0.07$

Table 3.1: Measurements of R_{K^*} for both the B^0 and B^+ modes in multiple q^2 bins by Belle collaboration [50]. The first (second) experimental errors are statistical (systematic).

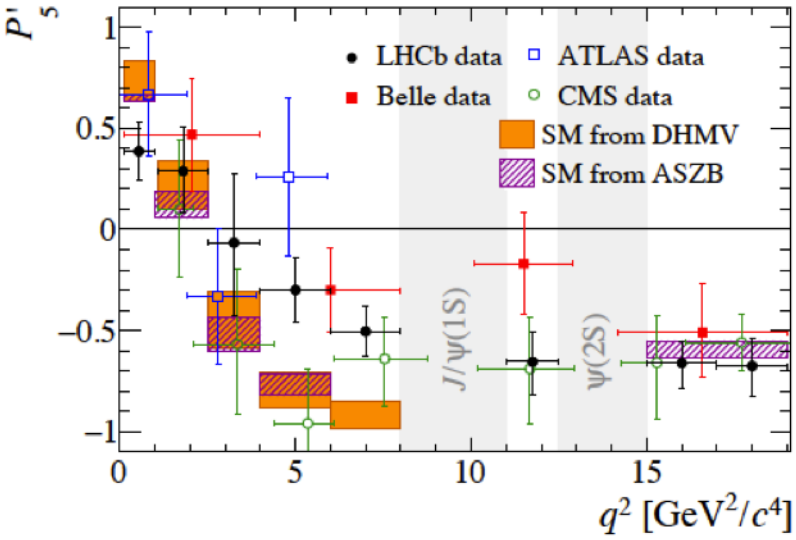

Figure 3.7: The P_5' anomaly [186].

These LFU anomalies can be explained by assuming new physics in muon, electron or both sectors. There are other anomalies which can be attributed to new physics in the muon sector only. The angular analysis of $B^0 \to K^{0*}\,\mu^+\,\mu^-$ decay provides a plethora of observables to probe new physics. Among these observables, P_5' is particularly interesting [165, 187]. The LHCb [41, 44] along with ATLAS [48] collaboration measured the value of P_5' in $4.0 \leq q^2 \leq 6.0$ GeV^2 bin. The measured value deviates from the SM prediction at 3.3σ level. The P_5' observable is also measured by the CMS and Belle collaborations in different q^2 bins. The CMS collaboration [46] measured P_5' in $4.3 \leq q^2 \leq 6.0$ GeV^2 bin which is consistent with the SM prediction. However, the measured value of P_5' by the Belle collaboration [45] in $4.3 \leq q^2 \leq 8.68$ GeV^2 bin is found to be 2.6σ away from the SM prediction. The measurements of P_5' by the LHCb, ATLAS, CMS and Belle collaborations, superimposed to the SM predictions, are represented in Fig. 3.7 [186].

Further, the LHCb collaboration reported several measurements of differential branching ratio and angular observables in $B_s \to \phi\,\mu^+\,\mu^-$ decay [40, 43]. Most of the measurements are consistent with the SM predictions. However, the differential branching ratio of this decay is found to be more than 3σ smaller than the SM prediction [188] in $1.0 \leq q^2 \leq 6.0$ GeV^2 bin. The SM prediction along with the experimental measurement of the differential branching ratio of $B_s \to \phi\,\mu^+\,\mu^-$ decay by the LHCb collaboration is shown in Fig. 3.8 [186].

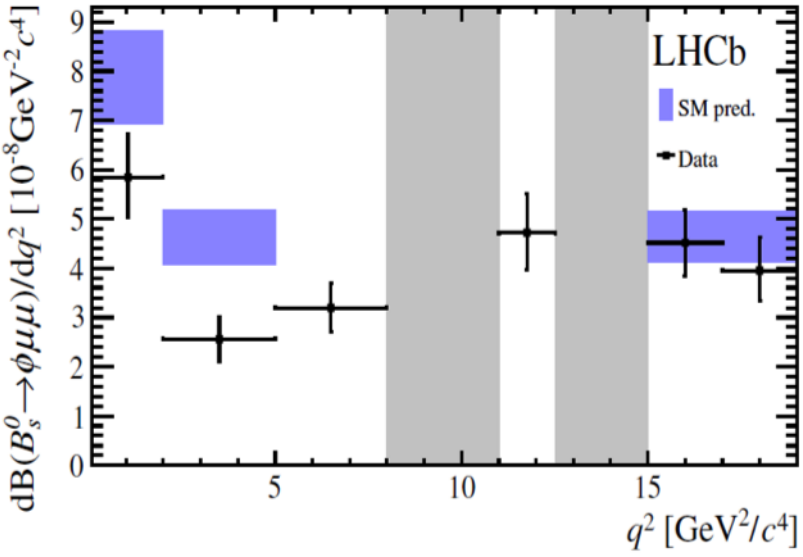

Figure 3.8: Anomaly in the branching ratio of $B_s \to \phi\,\mu^+\,\mu^-$ [186].

3.4 Anomalies in $b \to c\,l\,\bar{\nu}$ sector

The B-factories, BaBar and Belle, along with the LHCb collaboration have reported several measurements in the charged current transitions, which disagree with the predictions of the SM. Such decays are induced by the quark level transition $b \to c\,l\,\bar{\nu}$, which occurs at tree level in the SM. These discrepancies are an indication of LFU violation in the charged current sector:

$$R_D = \frac{\Gamma(B \to D\,\tau\,\bar{\nu})}{\Gamma(B \to D\,\{e/\mu\}\,\bar{\nu})}, \quad R_{D^*} = \frac{\Gamma(B \to D^*\,\tau\,\bar{\nu})}{\Gamma(B \to D^*\,\{e/\mu\}\,\bar{\nu})}. \tag{3.3}$$

The BaBar and Belle collaborations made precise measurements of these flavour ratios. Later on LHCb collaboration measured R_{D^*} and confirmed the discrepancy in 2017. After this measurement, the world averages of R_D and R_{D^*} exceeded the SM predictions by 2.3σ and 3.4σ respectively. Including the correlation, the tension was at the level of 4σ [189, 190]. In Moriond 2019, Belle collaboration updated these measurements which are in agreement with the SM predictions. With this update, the current world averages of R_D and R_{D^*} stand 1.4σ and 2.5σ away from their SM values. Considering the current correlation, the discrepancy is at 3.1σ [191, 192].

The SM predictions for these ratios along with the measured values are listed in Table 3.2. The disagreement of these measurements with SM predictions before and after Moriond 2019 are depicted in Fig. 3.9 and Fig. 3.10, respectively. These deviations indicate that the mechanism of $b \to c\,\tau\,\bar{\nu}$ decay is different from that of $b \to c\,\{e/\mu\}\,\bar{\nu}$. The LFU violation in $b \to c\,l\,\bar{\nu}$ sector is further corroborated by measurement of a new ratio related to the same quark level transition by the LHCb collaboration [60],

$$R_{J/\psi} = \frac{\Gamma(B_c \to J/\psi\,\tau\,\bar{\nu})}{\Gamma(B_c \to J/\psi\,\mu\,\bar{\nu})} = 0.71 \pm 0.17\,(\text{stat.}) \pm 0.18\,(\text{syst.}) \tag{3.4}$$

The measured value of $R_{J/\psi}$ is 1.7σ higher than its SM prediction 0.289 ± 0.010 [193]

Apart from these LFU ratios, the Belle collaboration has recently measured two angular observables in the decay $B \to D^*\,\tau\,\bar{\nu}$:

- τ polarization $P_\tau^{D^*}$
- D^* polarization fraction $f_L^{D^*}$

Experiment	R_{D^*}	R_D	Correlation(stat./syst./total)
BaBar [51, 52]	$0.332(24)(18)$	$0.440(58)(42)$	$-0.45/-0.07/-0.27$
Belle [54]	$0.293(38)(15)$	$0.375(64)(26)$	$-0.56/-0.11/-0.49$
Belle [55]	$0.302(30)(11)$	–	–
LHCb [53]	$0.336(27)(30)$	–	–
Belle [56, 58]	$0.270(35)^{(+28)}_{(-25)}$	–	–
LHCb [57, 59]	$0.291(19)(29)$	–	–
World average (2018) [189]	$0.304(13)(7)$	$0.407(39)(24)$	-0.20
Belle [61]	$0.283(18)(14)$	$0.307(37)(16)$	$-0.53/-0.51/-0.51$
World average (2019) [191]	$0.295(11)(8)$	$0.340(27)(13)$	$-0.39/-0.34/-0.38$
SM prediction [189]	$0.258(5)$	$0.299(3)$	–

Table 3.2: All measurements and the world averages of R_D-R_{D^*} along with their SM predictions. The first (second) experimental errors are statistical (systematic).

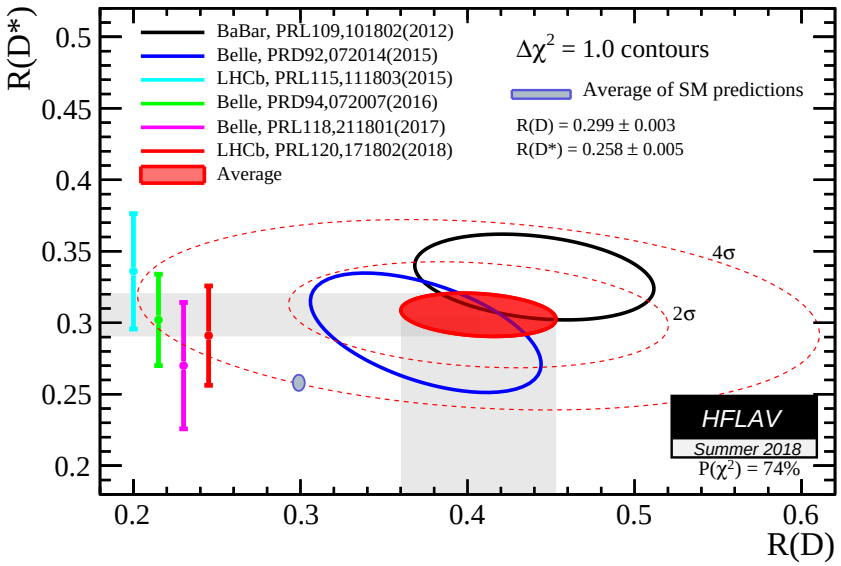

Figure 3.9: All measurements and the previous (2018) world average of R_D-R_{D^*} along with their SM predictions. Source: HFLAV Summer 2018 [190].

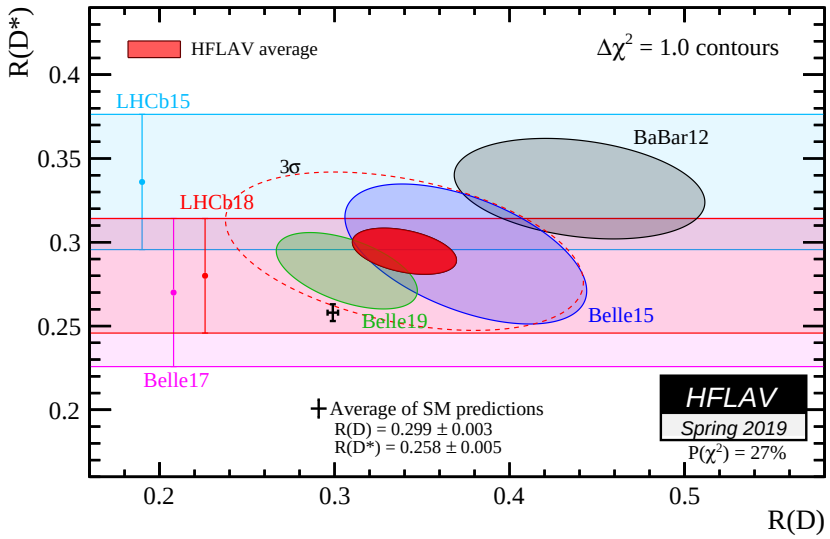

Figure 3.10: The present (2019) world average of R_D-R_{D^*}. Source: HFLAV Spring 2019 [192].

Using the full data sample of 772×10^6 $B\bar{B}$ pairs, the measured value of $P_\tau^{D^*}$ is $-0.38\pm0.51\,(\text{stat.})\,^{+0.21}_{-0.16}\,(\text{syst.})$ [56] which is consistent with its SM prediction -0.497 ± 0.013 [99]. Also, f_L is measured to be $0.60\pm0.08\,(\text{stat.})\pm0.04\,(\text{syst.})$ [194, 195]. The measured value of $f_L^{D^*}$ is somewhat higher than the the SM prediction 0.46 ± 0.04 [196]. Here, the disagreement is at the level of 1.5σ.

These discrepancies have drawn a lot of attentions from theoretical community. Several groups performed model independent analysis of these anomalies from which it was evident that there many new physics solutions which can account for these anomalous measurements. Therefore, one of the key open questions in flavour physics is to uniquely identify the Lorentz structure of possible new physics in these sectors. The primary goal of my thesis work is to address this problem by analyzing new observables in $b\to sl^+l^-$ sector. We also study correlations between $b\to c\tau\bar{\nu}$ and $b\to s\tau^+\tau^-$ in the context of $B_s^*\to\tau^+\tau^-$ decay. Further, we intend to study the effects of measurements in $b\to sl^+l^-$ sector to the top quark sector, in particular FCNC decay $t\to cZ$.